BIOCHEMISTRY
including biophysical chemistry & molecular biology

Article

pubs.acs.org/biochemistry

Specificity Determinants for Autoproteolysis of LexA, a Key Regulator of Bacterial SOS Mutagenesis

Charlie Y. Mo,[†] L. Dillon Birdwell,[‡] and Rahul M. Kohli*[,§,∥]

[†]Biochemistry and Molecular Biophysics Graduate Group, Perelman School of Medicine, University of Pennsylvania, 3610 Hamilton Walk, Philadelphia, Pennsylvania 19014, United States

[‡]Cellular and Molecular Biology Graduate Group, Perelman School of Medicine, University of Pennsylvania, 3610 Hamilton Walk, Philadelphia, Pennsylvania 19014, United States

[§]Department of Medicine and [∥]Department of Biochemistry and Biophysics, Perelman School of Medicine, University of Pennsylvania, 3610 Hamilton Walk, Philadelphia, Pennsylvania 19014, United States

Supporting Information

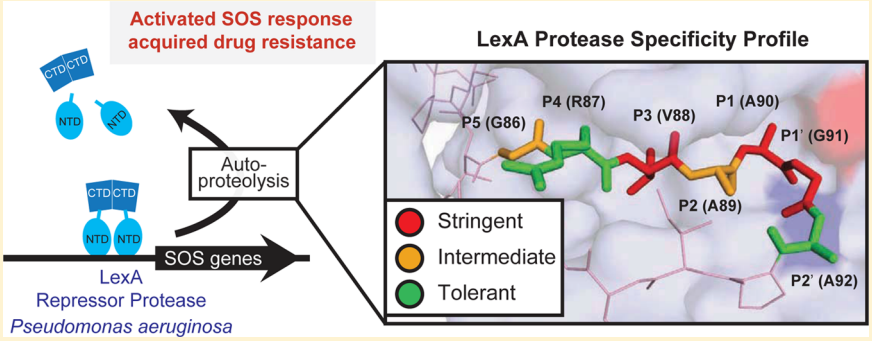

ABSTRACT: Bacteria utilize the tightly regulated stress response (SOS) pathway to respond to a variety of genotoxic agents, including antimicrobials. Activation of the SOS response is regulated by a key repressor-protease, LexA, which undergoes autoproteolysis in the setting of stress, resulting in derepression of SOS genes. Remarkably, genetic inactivation of LexA's self-cleavage activity significantly decreases acquired antibiotic resistance in infection models and renders bacteria hypersensitive to traditional antibiotics, suggesting that a mechanistic study of LexA could help inform its viability as a novel target for combating acquired drug resistance. Despite structural insights into LexA, a detailed knowledge of the enzyme's protease specificity is lacking. Here, we employ saturation and positional scanning mutagenesis on LexA's internal cleavage region to analyze >140 mutants and generate a comprehensive specificity profile of LexA from the human pathogen *Pseudomonas aeruginosa* ($LexA_{Pa}$). We find that the $LexA_{Pa}$ active site possesses a unique mode of substrate recognition. Positions P1−P3 prefer small hydrophobic residues that suggest specific contacts with the active site, while positions P5 and P1′ show a preference for flexible glycine residues that may facilitate the conformational change that permits autoproteolysis. We further show that stabilizing the β-turn within the cleavage region enhances LexA autoproteolytic activity. Finally, we identify permissive positions flanking the scissile bond (P4 and P2′) that are tolerant to extensive mutagenesis. Our studies shed light on the active site architecture of the LexA autoprotease and provide insights that may inform the design of probes of the SOS pathway.

In an era of rising drug resistance and a diminishing pipeline for new antibiotics, understanding the mechanisms that drive acquired drug resistance in bacteria has become critical. Bacterial adaptation and evolution are closely tied to the stress response (SOS) pathway, a widely conserved, inducible network of genes involved in DNA repair and recombination that allows bacteria to respond to DNA damage. The SOS response is governed by a bifunctional repressor-protease, LexA. In its basal state, LexA represses the transcription of 15−40 genes involved in the SOS response (Figure 1A). Interactions with RecA, a sensor of DNA damage, cause LexA to self-cleave (autoproteolyze), resulting in the derepression of the downstream SOS genes.[1−4] These induced SOS genes include Y-family DNA polymerases, which catalyze error-prone translesional replication over damaged DNA and can promote acquired drug resistance.[5,6] Further, LexA autoproteolysis increases the level of expression of integrons involved in the transfer of mobile genetic elements and has been associated with the formation of biofilms.[7,8] Thus, LexA and the SOS pathway regulate several of the major mechanisms by which pathogens can tolerate antimicrobials and acquire drug resistance.

The LexA repressor was the notable first of a family of enzymes shown to undergo self-cleavage as part of their

Received: January 7, 2014
Revised: April 11, 2014
Published: April 29, 2014

   dx.doi.org/10.1021/bi500026e | *Biochemistry* 2014, 53, 3158−3168

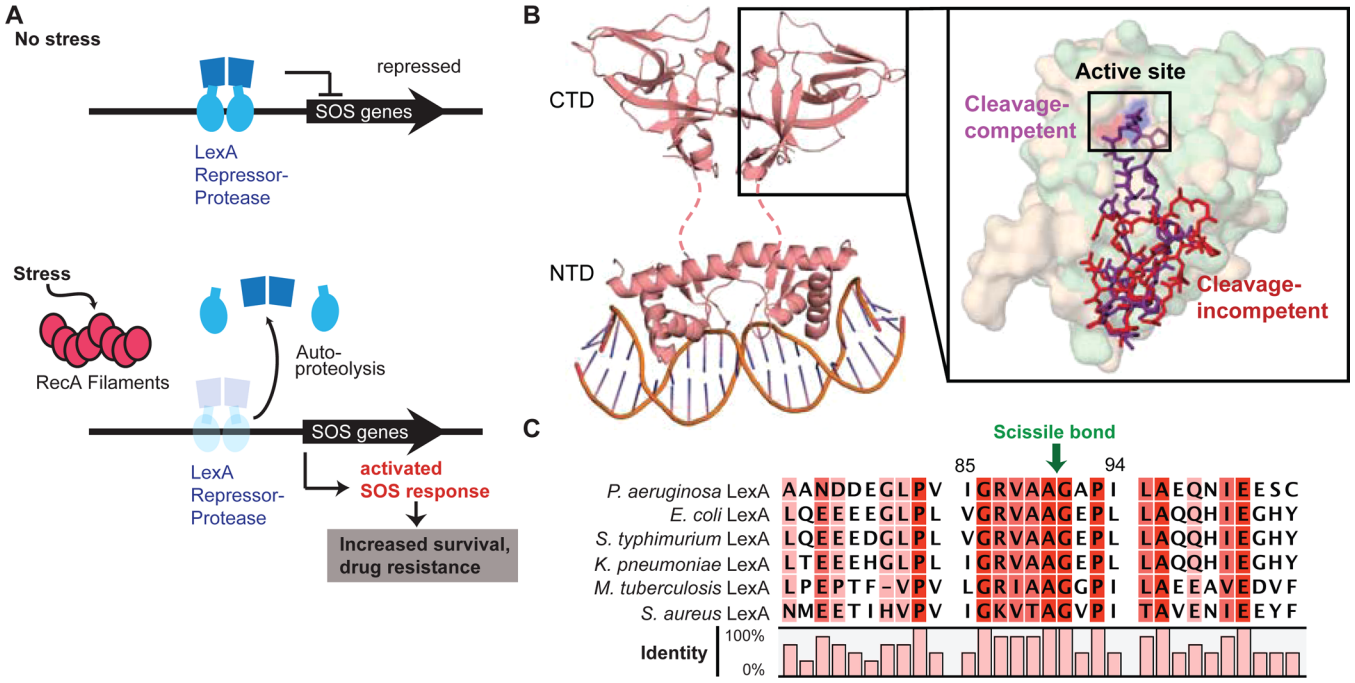

Figure 1. LexA repressor-protease regulates the bacterial stress response (SOS pathway). (A) Autoproteolysis of the LexA repressor-protease activates the mutagenic SOS response in bacteria. In the absence of stress, LexA binds to SOS-controlled promoters, limiting their action. When DNA is damaged, RecA filaments form at the site of damage and stimulate LexA self-cleavage. Autoproteolysis prompts dissociation of LexA from DNA, permitting expression of downstream SOS genes. Activation of the SOS response and its associated DNA damage tolerance pathways increases bacterial survival and mutation rates. (B) Structure of LexA from *E. coli*. LexA binds to DNA as a dimer. The C-terminal domain (CTD) contains the major dimerization interface and a serine protease active site. The N-terminal domain displays a winged helix−turn−helix motif and binds to the palindromic DNA of the SOS box. The CTD and NTD are connected by a flexible linker peptide (dashed line), which was not resolved in the crystal structure (PDB entry 3JSO). The close-up of the LexA CTD active site shows an overlay of the cleavage-competent and cleavage-incompetent forms of LexA (PDB entries 1JHE and 1JHC, respectively). The internal cleavage loop of LexA undergoes a large conformational change between the cleavage-incompetent state (red) and the cleavage-competent state (purple), placing a scissile bond in the proximity of the active site serine-lysine catalytic dyad (red and blue surfaces, respectively). The active site is boxed for the sake of clarity. (C) The LexA cleavage regions across species from different families of pathogenic bacteria (Gram-negative, Gram-positive, and mycobacteria) are shown. The scissile Ala-Gly bond is noted (green arrow), and numbering is shown relative to *Pseudomonas aeruginosa* LexA ($LexA_{Pa}$). The percent identity is represented by the degree of shading with red and plotted below the alignment.

physiological function.[9−15] Members of this family possess a conserved serine-lysine catalytic dyad that cleaves between an Ala-Gly or Cys-Gly sequence within the protease domain.[12] In its repressor role, LexA functions as a dimer, with each monomer containing an N-terminal DNA binding domain (NTD) that is connected by a flexible linker to the C-terminal serine protease domain (CTD) (Figure 1B).[16] Structural studies of *Escherichia coli* LexA have shown that the CTD can exist in two distinct conformations, and that self-cleavage is associated with a shift from a basal cleavage-incompetent conformation of the CTD to a cleavage-proficient conformation.[12,16] Self-cleavage is initiated when LexA is exposed to either activated RecA (RecA*) *in vivo* and *in vitro* or high pH *in vitro*, features shared by several other members of the LexA superfamily.[9−11,17,18]

The cleavage-proficient conformation of LexA has several unique features. The protein loop containing the scissile Ala-Gly bond appears to form specific contacts near the active site, suggesting that like classical serine proteases, there is a binding pocket involved in cleavage sequence recognition.[12] Indeed, genetic mutagenesis and selection studies of LexA and the related λ CI repressor have indicated that point mutations at several of the residues surrounding the cleavage loop can interfere with self-cleavage.[19−21] However, in conventional serine proteases, the scissile bond of the substrate peptide is almost uniformly bound in the middle of an extended β-sheet. In LexA, by contrast, the bond is positioned at the end of a β-turn.[12,22−24] Furthermore, because LexA acts upon a tethered substrate (the cleavage region within the same molecule), the effective local concentration of the substrate is high. This feature may explain why common serine protease inhibitors, such as diisopropyl fluorophosphate, inhibit LexA only at extremely high concentrations, and why wild-type LexA only weakly cleaves peptides or other proteins *in trans*.[18,25] This distinctive binding mode and requirement for a conformational change for catalysis make LexA a potentially distinctive therapeutic target among proteases.

Genetic and synthetic biology studies have shown that preventing LexA autoproteolysis decreases the rate of development of resistance and can sensitize bacteria to antibiotics. Most notably, when an *E. coli* strain harboring a noncleavable mutant of LexA was evaluated in a murine infection model, the development of antibiotic resistance was abrogated by the loss of normal LexA function.[26] Specifically, while the wild-type bacteria thrived and became entirely resistant to rifampin after drug exposure in the mouse model, the mutant strain failed to acquire any rifampin resistance. In an alternative study, phage-mediated transduction of *E. coli* with an inactivated LexA protease was shown to greatly hypersensitize the bacteria to traditional antibiotics.[27] In addition to participating in the

dx.doi.org/10.1021/bi500026e | *Biochemistry* 2014, 53, 3158−3168

transfer of mobile genetic elements, LexA has been suggested to mediate persister formation and play a role in stress-induced mutagenesis.[7,28,29] Targeting LexA pharmacologically, therefore, has been suggested as a means to delay the acquisition of resistance, increase the efficacy of known antimicrobials, and offer insight into bacterial adaptation and evolution.[26,30,31]

Despite the availability of crystal structures of the LexA, a detailed structure−function relationship of the LexA active site and the cleavage sequence has yet to be established. Here, we study the LexA protein from *Pseudomonas aeruginosa* ($LexA_{Pa}$), a Gram-negative pathogen that is an archetype for the problem of acquired drug resistance and a major cause of mortality in cystic fibrosis patients.[32,33] We developed a methodology for high-efficiency mutagenesis and enzymatic characterization to profile the substrate preferences of LexA autoproteolysis comprehensively for the first time. Combined with available structural data, this study provides insight into the mechanism of LexA substrate recognition and lays the groundwork for efforts to develop inhibitors and probes of LexA, the SOS pathway, and bacterial evolution.

EXPERIMENTAL PROCEDURES

$LexA_{Pa}$ Cloning and Expression. All oligonucleotide sequences used in $LexA_{Pa}$ amplification, cloning, and cassette mutagenesis were purchased from Integrated DNA Technologies (IDT) and are available upon request. The *lexA* gene was amplified via polymerase chain reaction with $LexA_{Pa}$ genomic primers from the *P. aeruginosa* PA01 strain and cloned into the pET41 expression vector engineered with an N-terminal His tag and C-terminal Streptavidin tag.[34] The S125A active site mutant was generated by QuikChange site-directed mutagenesis. The enzyme was heterologously expressed in *E. coli*, followed by one-step purification using the N-terminal tag. The purified product was predominantly full-length (∼26 kDa), with trace amounts of self-cleavage that occurs during the course of purification.

Saturation Mutagenesis. For the efficient generation of saturation and positional scanning mutagenesis variants, mutations introducing the unique restriction sites AgeI and EagI were engineered at nucleotide positions 255 and 282, respectively, in the *lexA* coding sequence using QuikChange site-directed mutagenesis. An additional mutation (*Bam*HI) at nucleotide 267 and a TAG stop were included within the cassette region, as mechanisms for selection against wild-type sequences from the parent vector. This construct served as the parent cloning vector for cassette-based mutagenesis. Briefly, the $LexA_{Pa}$ cloning vector was digested with AgeI, BamHI, and EagI for 2 h at 37 °C and treated with calf intestinal phosphatase. Individual oligonucleotides containing a degenerate codon (NNS) at each position from position 85 to 94 were ordered from IDT and annealed to their complement with a standard annealing protocol. Annealed oligonucleotides containing sticky ends complementary to AgeI and EagI cleavage sites were phosphorylated with T4 polynucleotide kinase for 1 h at 37 °C. The oligonucleotide cassettes were ligated into the digested cloning vector using T4 DNA ligase. The ligation product was then transformed into New England Biolabs (NEB) 10-β competent cells using standard transformation procedures. One-tenth of the transformation mixture was plated to estimate the library size, and the remaining portion was grown overnight in Luria-Bertani broth. The isolated plasmids from this culture constituted the saturation mutagenesis library at each position (I85X, G86X, etc.). Successful incorporation of the degenerate NNS codon was verified by Sanger sequencing of the library.

Point Mutations of Selected Residues in the $LexA_{Pa}$ Cleavage Loop. The same cassette-based mutagenesis strategy was adopted to generate the individual point mutations in residues spanning positions P5 to P2′ of the $LexA_{Pa}$ cleavage region (residues 86−92). For each of the seven positions, 20 forward and reverse oligonucleotides encoding each amino acid mutation were constructed and ordered from IDT. Oligonucleotides containing two mutant codons were used for the $LexA_{Pa}$ A89C/I94C double mutant. Oligonucleotide pairs were annealed, phosphorylated, and ligated into the digested parent vector, as described above. After transformation, individual colonies were selected and mutant plasmids were sequenced to confirm the proper insertion of the mutation cassettes.

Expression and Purification of $LexA_{Pa}$, Saturation Mutant Cohorts, or Individual Positional Scanning Mutants. Expression plasmids were transformed into BL21-(DE3)-pLysS *E. coli* cells for heterologous expression. For the saturation mutant library, the liquid culture after transformation was used as the starter overnight culture. For point mutants, the transformation was plated and an individual colony selected for the starter overnight culture. The following day, 35 mL Luria-Bertani broth cultures were inoculated with 1 mL of overnight culture and grown at 37 °C until the OD_{600} reached ∼0.6. The cultures were subsequently induced with 1 mM isopropyl β-D-1-thiogalactopyranoside, shifted to 30 °C, and grown for 4 h. The culture was centrifuged at 4000 rpm for 20 min at 4 °C and the pellet stored at −80 °C until it was purified. Thawed cell pellets were lysed per protocol with Bugbuster Mastermix (Novagen). The soluble supernatant was incubated with 100 μL of reconstituted HisPur resin (Pierce) for batch binding at 4 °C for 1 h in 10 mL polyprep columns (Bio-Rad). The flow-through was discarded and the resin subsequently washed three times with 10 resin volumes of wash buffer [25 mM sodium phosphate (pH 7.0), 150 mM NaCl, and 30 mM imidazole]. Following the wash, bound protein was eluted from the resin with 3 resin volumes of elution buffer [25 mM sodium phosphate (pH 7.0), 150 mM NaCl, and 200 mM imidazole]. The eluted proteins were then dialyzed into 25 mM Tris-HCl (pH 7.0), 150 mM NaCl, and 10% glycerol. The same protocol was used for the wild-type enzyme, saturation mutant libraries, and individual positional scanning mutants. For the 140 positional scanning mutants (20 amino acids × 7 positions), the cohorts of 20 mutants at each position were processed in parallel to provide an internal (wild-type) control.

Alkali-Mediated Qualitative Cleavage Assays of $LexA_{Pa}$. To qualitatively screen the cleavage ability of $LexA_{Pa}$ variants, purified protein was mixed in a 1:1 ratio with 2× cleavage buffer (100 mM Tris-Glycine-CAPS and 300 mM NaCl) at pH 7.2 or 10.6. Reaction mixtures were incubated at room temperature for 16 h. Cleavage was quenched by adding 2× Laemmli sample buffer to the reaction mixture and by denaturation at 95 °C for 10 min. The extent of $LexA_{Pa}$ cleavage was visualized by running reaction samples on 15% sodium dodecyl sulfate−polyacrylamide gel electrophoresis (SDS−PAGE) gels and Coomassie staining. Mutants that displayed cleavage were selected for further quantitative analysis. Coomassie-stained gels were imaged on a Typhoon Imager using red laser excitation at 633 nm and no filters. The fraction of cleaved protein was calculated by dividing the density of the $LexA_{Pa}$ cleavage products by the sum of the density of all $LexA_{Pa}$ full-length and cleaved components, using

Quantity One (Bio-Rad). Linear detection of Coomassie-stained products was verified by analysis of standards.

RecA*-Mediated Cleavage of LexA$_{Pa}$ Proteins. RecA of *E. coli* was purchased from NEB. Purified LexA$_{Pa}$ was incubated with an excess of activated RecA*, generated by premixing ~100 μg/mL RecA, 900 μM ATPγS, and 10 μM ssDNA.[35] Reactions without RecA were run parallel as a negative control. Reaction mixtures were incubated at room temperature for 16 h. The cleavage products were analyzed and quantified as described for alkali-mediated cleavage.

Alkali-Mediated Quantitative Assays of LexA$_{Pa}$. For quantitative kinetic analysis, 25 μL of purified protein was mixed with 25 μL of 2× cleavage buffer (pH 10.6) and the mixture incubated at 37 °C for 2 h. At the given time points, 5 μL of the reaction mixture was removed and the reaction rapidly quenched in 2× Laemmli sample buffer. The extent of cleavage over time was visualized on Coomassie-stained 15% SDS−PAGE gels. For restrictive positions, time points were collected in triplicate, while reactions were run in duplicate for the permissive positions. Coomassie-stained gels were imaged and quantified as detailed above.

Calculation of LexA$_{Pa}$ Cleavage Rates and Generation of the LexA$_{Pa}$ Cleavage Profile. The density of the protein bands was quantified using Quantity One (Bio-Rad). For each time point, the fraction of uncleaved LexA$_{Pa}$ was calculated as described above and plotted versus time. Rate plots were then fit to the first-order exponential decay equation $A = A_0e^{-kt}$ using Prism to obtain k, the observed rate of cleavage. To calculate the specificity profile, we used the enoLOGOS web tool to generate a normalized sequence LOGO of the P5−P2′ sequence preferences.[36] The cleavage rate constants, k, at each position were used as the relative scaling factors, with an unknown weight type and the frequency method for calculating the height of the symbol stacks.

Structural Modeling of LexA$_{Pa}$. To assist with the analysis of our biochemical data, we generated a structural model of the LexA$_{Pa}$ CTD. We entered the amino acid sequence of the LexA$_{Pa}$ CTD (residues 81−204) into Modeler 2.0,[37] with the crystal structure of activated LexA from *E. coli* as the homology template (PDB entry 1JHE).[12]

Liquid Chromatography and Tandem Mass Spectrometry (LC−MS/MS). LC−MS/MS was performed at the Proteomics & Systems Biology Core Facility at the University of Pennsylvania Perelman School of Medicine. Purified LexA$_{Pa}$ A89C/I94C samples were either reduced or not reduced with 1 M dithiothreitol and treated with 300 mM iodoacetamide (molecular mass of 57 Da). Samples were subsequently digested with trypsin and subjected to LC−MS/MS. Peptide fragments were identified and analyzed with PEAKS.[38]

RESULTS

The Sequence of LexA$_{Pa}$ Is Strongly Identical to That of LexA of *E. coli*. The LexA protein is strongly conserved across all families of bacteria and shares a high level of sequence similarity.[9−15] Given the importance of drug resistance in the opportunistic pathogen *P. aeruginosa*, we focused our efforts on studying the LexA of *P. aeruginosa* (LexA$_{Pa}$). A sequence alignment of LexA$_{Pa}$ with LexA of *E. coli* (LexA$_{Ec}$) reveals a 64% sequence identity, with notable features such as the serine-lysine catalytic dyad and the internal cleavage loop conserved (Figure S1A of the Supporting Information). This strong sequence identity provided the basis for structural modeling of the LexA$_{Pa}$ CTD to help interpret our biochemical assays (Figure S2 of the Supporting Information). We modeled LexA$_{Pa}$ based on the structure of the CTD of LexA$_{Ec}$ in the active conformation (PDB entry 1JHE), with the high degree of sequence homology resulting in a root-mean-square deviation of 1.2 Å between the known and modeled structures.

Saturation Mutagenesis of LexA$_{Pa}$ Reveals the Tolerance of Residues in the LexA Cleavage Region to Mutation. We next cloned, expressed, and purified LexA from reference strain PA01. In accordance with prior biochemical assays on LexA from other species, we demonstrated that our tagged LexA$_{Pa}$ is proficient in both alkali- and RecA*-mediated autoproteolysis (Figure S3 of the Supporting Information). Recombinant LexA$_{Pa}$ displayed cleavage kinetics similar to that of tagged or untagged LexA from other species (see below).[18,39−42]

Prior biochemical studies have revealed that the LexA protease has poor cleavage activity *in trans*.[18,25] In its wild-type catalytic form, both the full-length LexA protein and the isolated LexA protease domain are unable to efficiently cleave the target substrate of a second LexA enzyme.[18] Extensive mutagenesis of the enzyme's active site and the target sequence can allow for trace detectable activity *in trans*; however, it is clear that the native substrate of LexA is itself.[18] We explored the possibility that full-length LexA or the CTD alone may cleave short peptides that mimic the internal cleavage loop; however, we did not observe cleavage in fluorescence- or LC−MS-based cleavage assays (data not shown). For these reasons, conventional peptide array-, genetic library-, and mass spectrometry-based methods for assessing protease specificity could not be readily translated to characterizing LexA$_{Pa}$ specificity.[43−47] We therefore decided to directly assess LexA's specificity by exhaustive mutagenesis of the cleavage loop within the enzyme and assessing (in *cis*) autoproteolysis activity. Given that this approach would require extensive mutagenesis, we implemented an efficient cassette mutagenesis strategy for introducing variations into the internal substrate of LexA (Figure S4 of the Supporting Information).[48−50] The specificity determinants of LexA$_{Pa}$ could be delineated broadly at first by saturation mutagenesis (the introduction of a degenerate codon) and then in detail by positional scanning mutagenesis (the generation of individual point mutants to each of the 20 amino acids).

For saturation mutagenesis, 10 duplexed oligonucleotide cassettes that contain a degenerate NNS codon at each position from Ile85 to Ile94 (e.g., I85X) were produced. The degenerate NNS codon encodes all 20 potential amino acid variants and one potential stop codon (TAG). The calculated depth of the library at each position was >1000-fold, and the presence of a degenerate NNS codon at each position was verified by sequencing. Although this library is not proportionally represented for the various amino acid substitutions, we reasoned that the general patterns of restrictive and permissive positions could be gleaned from analysis of a positionally diversified cohort of variants.

For each position, we expressed and purified the mutant protein library in cohort, which showed expression characteristics and solubility similar to those of wild-type LexA$_{Pa}$. Each cohort was then incubated overnight at pH 7.2 or 10.6, and the fraction of cleavage was assessed under these conditions (Figure 2). The positions clustered into two general groups based upon comparison to wild-type LexA$_{Pa}$: positions P5 (G86), P3 (V88), P2 (A89), P1 (A90), and P1′ (G91) appear to be restrictive to mutation, displaying small changes in the

dx.doi.org/10.1021/bi500026e | *Biochemistry* 2014, 53, 3158−3168

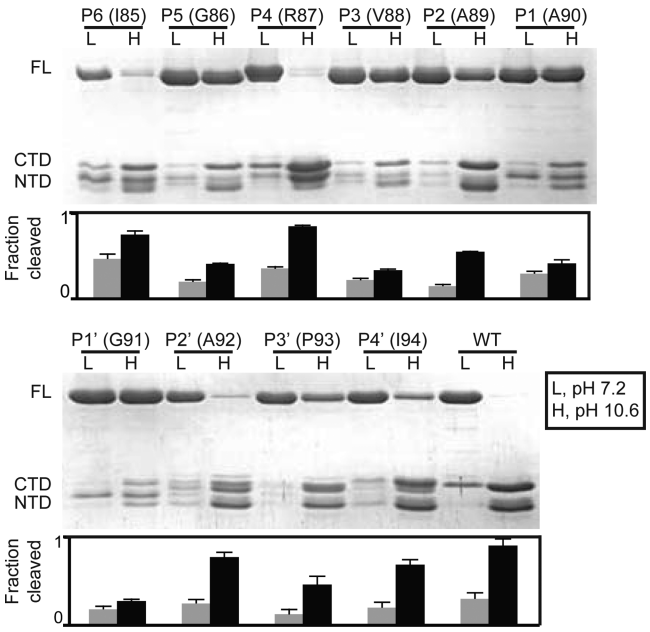

Figure 2. Saturation mutagenesis of the $LexA_{Pa}$ cleavage region. For each position from I85 to I94, the wild-type codon was substituted with a degenerate NNS codon. To determine the tolerance for mutation at each position qualitatively, the saturation mutant library at each position was purified as a cohort and subjected to overnight self-cleavage at pH 7.2 (L) or pH 10.6 (H). Self-cleavage of the full-length (FL) enzyme results in the generation of the isolated C-terminal and N-terminal domains (CTD and NTD, respectively). The multiple banding in the lower-molecular weight fragments is caused by the migration patterns of mutants with an altered charge state. The fraction of cleavage product detected under each condition is shown (pH 7.2, gray columns; pH 10.6, black columns). Error bars represent the standard error of duplicate trials.

fraction of cleaved protein (<30%), while the remaining positions were more permissive to the introduction of a degenerate codon, exhibiting changes in cleavage levels closer to that of the wild-type enzyme despite being highly diversified (Figure 2). We repeated the analysis in the presence or absence of RecA* and found the same overall patterns of tolerant and restrictive positions with this alternative stimulus for autoproteolysis (Figure S5 of the Supporting Information). Notably, as RecA*-mediated cleavage analysis was used as a purely qualitative measure, we used RecA from *E. coli* in our assays (74% identical and 87% similar to that of *P. aeruginosa*) because of its availability and the observation that $LexA_{Pa}$ cleaves as efficiently as $LexA_{Ec}$ under RecA* stimulation.

Positional Scanning Mutagenesis and a Cleavage Screen of Residues P5−P2′ Identify Specific Residues That Are Important for $LexA_{Pa}$ Autoproteolysis. The qualitative overview from saturation mutagenesis set the stage for detailed quantitative analysis. Here, we focused on the residues of positions P5−P2′, spanning the most restrictive sites we identified by saturation mutagenesis. Furthermore, the $LexA_{Pa}$ homology model suggests that these residues form the most extensive interactions with the surrounding active site pocket (Figure S2 of the Supporting Information).

In our positional scanning mutagenesis approach, for each position of interest, we individually mutated the residues to each of the 20 potential amino acids (G86A, G86S, G86T, etc.) using cassette mutagenesis. For each position, all 20 variants were expressed, purified in parallel and subjected to both alkali- and RecA*-mediated cleavage overnight to identify specific variants that permitted autoproteolysis (Figure S6 of the Supporting Information). Together, the individual point mutants in this assay validated the patterns observed with saturation mutagenesis. The full cleavage profiles for each position are provided in Figure S6 of the Supporting Information, with select examples of a restrictive and tolerant position shown in Figure 3. Restrictive positions, such as P1 (A90), tolerate only a few mutations, while permissive positions, such as P4 (R87), tolerated all amino acids, although to varying degrees (Figure 3). Both alkali- and RecA*-mediated cleavage screens yielded similar cleavage results, with the exception of position P5, where RecA*-mediated cleavage was more restrictive than alkali-mediated cleavage (Figure S6A of the Supporting Information). Overall, the cleavage behavior of select restrictive mutations in $LexA_{Pa}$ (G86V, G86D, V88M, V88E, A89V, A90D, and A90T) agrees qualitatively with the results of a prior study of LexA from *E. coli* that identified slow-cleaving variants via limited mutagenesis and genetic screening.[51] One notable exception is the aspartate mutation at the P1′ glycine, which completely abrogates alkali-mediated and RecA*-mediated cleavage in $LexA_{Pa}$ (Figure S6F of the Supporting Information) but allows limited levels of cleavage in LexA from *E. coli*.[51]

Kinetic Evaluation of Cleavable Mutants. Individual mutants deemed cleavage-proficient under overnight cleavage conditions were next subjected to detailed kinetic analysis. We performed the cleavage reaction under alkali-induced conditions to allow for direct comparison of the various mutants. Alkali-mediated cleavage, while nonphysiological, has the distinctive advantage of being a unimolecular first-order reaction, allowing us to probe the intrinsic substrate preferences of $LexA_{Pa}$ without confounders such as potential alterations in RecA* interactions (Table 1). Employing our method, we determined the rate of autoproteolysis of all cleavable mutants. Representative data from one highly restrictive (P1) position and one tolerant position (P4) are presented in panels C and D of Figure 3, with kinetic plots for all cleavable variants shown in Figure S7 of the Supporting Information. Notably, the rate of cleavage of the wild-type enzyme at each position differed slightly (range of $53-144 \times 10^{-5}$ s^{-1}) as a result of batch-to-batch variability in expression and purification. Given that each cohort of 20 mutants at a position was prepared in parallel, the rate of each mutant was scaled to that of the wild type to obtain the relative amino acid preferences, with the comprehensive analysis summarized (Figure 4A).

The positions upstream of the cleavage site show an alternating pattern of being restrictive or permissive to variation, with restrictive positions favoring the wild-type residue over all other amino acids. At position P5 (G86), we see a modest tolerance for amino acids with either a small or flexible side chain, such as A or S, while larger side chains reduce the level of $LexA_{Pa}$ self-cleavage (Figure 4B). Position P4 (R87), which appears solvent-exposed in the $LexA_{Pa}$ model, shows tolerance to all variants, despite being conserved as a basic residue across species (Figure 1C). Indeed, certain acidic or large hydrophobic variants such as R87E and R87W appear to cleave at rates higher than that of the wild-type enzyme. Position P3 (V88) is restrictive, with the wild-type residue preferred 5-fold over the next best variant, V88I. Three of the four best variants are the β-branched amino acids, suggesting the possibility of active site engagement with the branched side chains. Other tolerated variants are hydrophobic and

dx.doi.org/10.1021/bi500026e | *Biochemistry* 2014, 53, 3158−3168

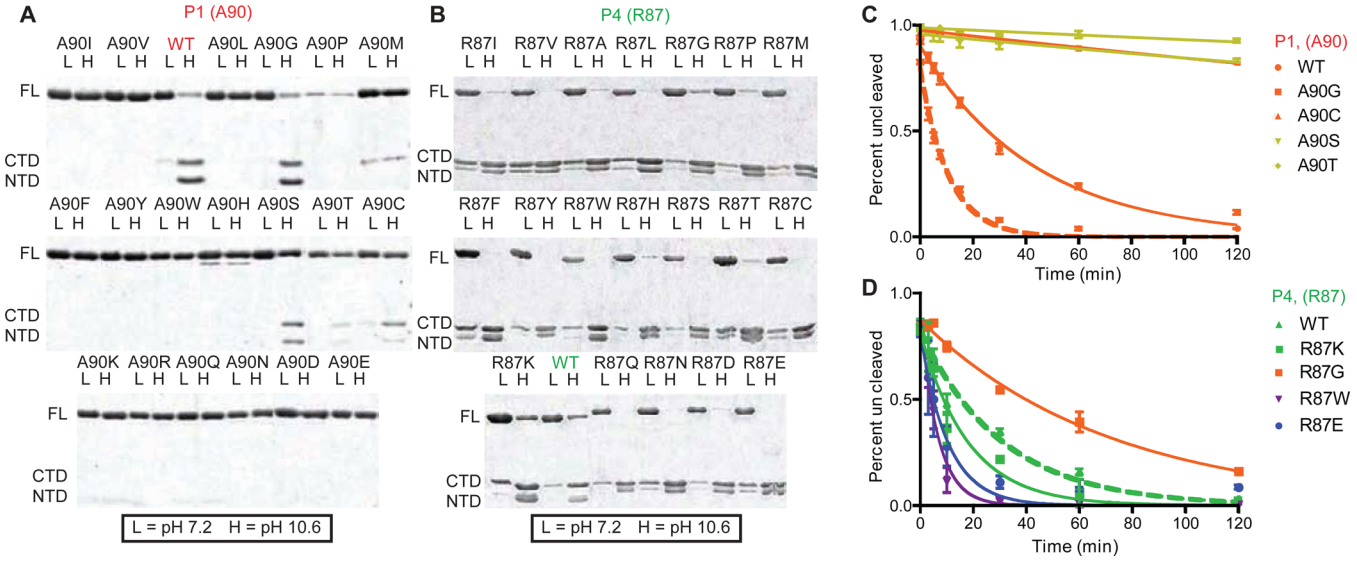

Figure 3. Positional scanning mutagenesis and kinetic analysis of the LexA$_{Pa}$ cleavage region. Each residue from G85 to A92 was mutated to each of the 20 amino acids. Each point mutant was expressed and purified separately. Shown are the results from overnight cleavage at pH 7.2 (L) or pH 10.6 (H) for each mutant of (A) A90 (position P1), a relatively restrictive position, or (B) R87 (position P4), a relatively tolerant position. The wild-type enzyme is denoted by WT. Cleavable mutants of (C) A90 (position P1) or (D) R87 (position P4) from the initial cleavage screen were then evaluated for their alkali-stimulated cleavage kinetics. The data represent three replicates for restrictive (P1) positions and two replicates for tolerant (P4) positions. For the sake of clarity, the kinetic data for five of the 20 R87 variants representing varying cleavage rates are shown. The points are fit as a first-order exponential decay, and the standard error is shown. Mutants are grouped by the properties of their side chains at physiological pH (orange for hydrophobic, purple for aromatic, yellow for hydrophilic, green for positive charge, and blue for negative charge). The wild-type (WT) residue is indicated with a thicker dotted line. Corresponding results for all positions from P5 to P2′ are displayed in Figures S6 and S7 of the Supporting Information, with quantitative results for rates listed in Table 1.

Table 1. First-Order Rate Constants for Alkali-Induced Self-Cleavage of LexA$_{Pa}$ Mutants

	rate, k ($\times 10^{-5}$ s^{-1})						
	P5	P4	P3	P2	P1	P1′	P2′
amino acid mutation	G86	R87	V88	A89	A90	G91	A92
G	76 ± 13	23 ± 2	3.2 ± 0.2	113 ± 8	38 ± 2	144 ± 3	26 ± 2
A	25 ± 2	143 ± 10	10.5 ± 0.8	98 ± 3	157 ± 10	-	95 ± 13
S	11 ± 1	85 ± 10	0.5 ± 0.1	121 ± 8	2.0 ± 0.3	2.8 ± 0.3	50 ± 3
C	3.8 ± 0.3	63 ± 10	5.5 ± 0.5	4.0 ± 0.5	2.3 ± 0.2	–	105 ± 10
T	2.8 ± 0.3	130 ± 17	8.7 ± 0.5	3.0 ± 0.5	1.0 ± 0.2	–	53 ± 7
D	7.8 ± 0.2	63 ± 7	–	2.2 ± 0.3	–	–	27 ± 2
P	–	103 ± 12	–	3.2 ± 0.5	–	–	433 ± 150
N	15.8 ± 0.3	45 ± 8	–	6.5 ± 0.5	–	–	137 ± 12
V	0.5 ± 0.2	113 ± 20	76 ± 7	1.0 ± 0.1	–	–	62 ± 5
E	3.8 ± 0.1	183 ± 33	–	2.2 ± 0.3	–	–	85 ± 8
Q	2.5 ± 0.2	100 ± 17	–	5.5 ± 0.8	–	–	167 ± 20
H	7.3 ± 0.2	25 ± 5	–	5.2 ± 1.2	–	–	85 ± 7
L	0.5 ± 0.2	45 ± 7	0.16 ± 0.01	4.8 ± 0.3	–	–	73 ± 5
I	7.8 ± 0.2	50 ± 8	15.2 ± 0.7	2.2 ± 0.2	–	–	125 ± 12
M	11 ± 2	60 ± 7	0.3 ± 0.1	2.2 ± 1.2	–	–	65 ± 5
K	6.0 ± 0.2	78 ± 10	–	1.3 ± 0.3	–	–	103 ± 10
F	5.8 ± 0.3	68 ± 10	–	6.8 ± 1.0	–	–	75 ± 12
Y	6.5 ± 0.3	210 ± 45	–	9.0 ± 1.3	–	–	65 ± 5
R	3.2 ± 0.2	53 ± 3	–	4.7 ± 0.2	–	–	77 ± 13
W	5.5 ± 0.2	216 ± 12	–	25 ± 3	–	–	113 ± 15

predominantly small amino acids. Position P2 (A89), exposed in the active conformation of LexA$_{Pa}$, tolerates all amino acids, although to different extents. Variants with the smallest side chains (A89G, wild type with A89, and A89S) are most readily cleaved, while the level of cleavage generally decreases as a function of increasing size.

The positions immediately flanking the cleavage site show highly restrictive patterns, while preferences are again relaxed in the downstream positions. At position P1 (A90), only the five smallest amino acids are tolerated: the wild-type A90 is preferred over the next best variant A90G by 4-fold, while cleavage is detectable with A90C, A90S, and A90T, suggesting significant active site constraints at this position. Position P1′

dx.doi.org/10.1021/bi500026e | Biochemistry 2014, 53, 3158−3168

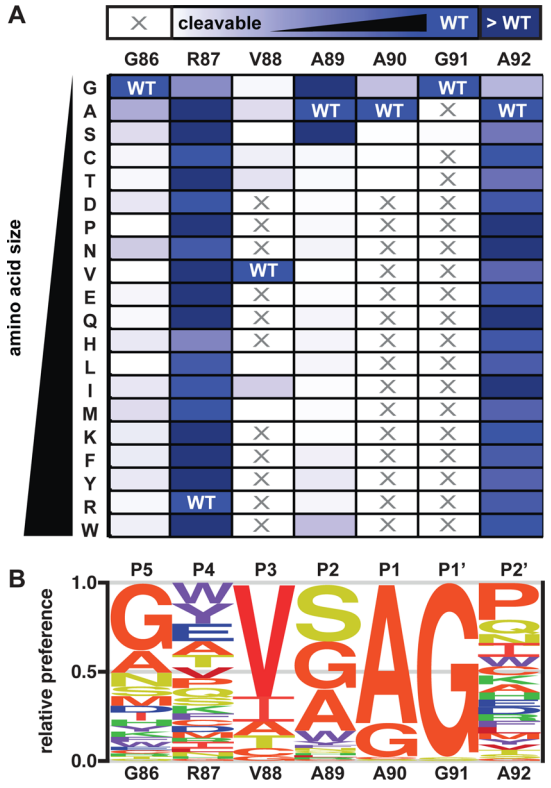

Figure 4. Substrate preference for alkali-mediated self-cleavage of $LexA_{Pa}$. (A) Heat map representing the cleavage rates of the $LexA_{Pa}$ point mutants. The wild-type residues from position P5 to P2′ are listed along the top. The rows represent each point mutation, listed in order of the increasing size of the amino acid. Crosses denote analogues that show no cleavage in the overnight self-cleavage assay at pH 10.6. For each cleavable analogue, the first-order rate constant for self-cleavage was determined at pH 10.6 [two or three replicates per condition (Table 1)]. The rate for each mutant was scaled relative to the wild-type residue and shown in the heat map as shades from white to blue. Residues that cleave at rates greater than that of the wild type are colored deep blue. (B) Normalized sequence LOGO diagram summarizing the autoproteolysis profile of $LexA_{Pa}$. The diagram was generated using the enoLOGOS program with the rates of cleavage at each position as the relative scaling factors. The color scheme groups amino acids as in Figure 3.

(G91) is situated at the β-turn of the LexA cleavage region in its active conformation. It is the most restrictive position among those examined, with only a serine mutation retaining any detectable self-cleavage activity (~50-fold slower than the WT). Position P2′ (A92) is a solvent-exposed residue and situated at the end of the β-turn. The tolerance of this position to mutation is in line with its poor conservation across species isoforms of LexA (Figure 1C).

The kinetic data determined at each position allow for the construction of the overall sequence preference heat map for $LexA_{Pa}$ (Figure 4A). The calculated cleavage rates were used to build the position-specific scoring matrix, which was then graphically converted into a sequence LOGO depiction that encapsulates the substrate specificity profile for $LexA_{Pa}$ (Figure 4B). As evidenced in the sequence LOGO, positions tolerant to mutation have high entropy or variability, while restrictive positions show low variability.

Kinetic Analysis Reveals $LexA_{Pa}$ Mutants That Cleave Faster than the Wild-Type Enzyme. In our kinetic assays of the $LexA_{Pa}$ mutants, we observed that certain mutants interestingly exhibited a cleavage rate higher than that of the wild-type enzyme ("hyperactive" mutants). While some hyperactive mutants of LexA have previously been discovered through genetic screens,[52,53] the molecular basis for hyperactive self-cleavage has not been well-investigated. In our mutagenesis, A92P shows a notable cleavage rate ~4-fold higher than that of the wild-type enzyme and undergoes autoproteolysis even under nonstimulatory conditions (neutral pH, no RecA*) (Table 1 and Figure S6G of the Supporting Information). The transition between the cleavage-incompetent and cleavage-competent forms of LexA is associated with a β-turn at the cleavage site (A90-G91).[12] Because position A92 is located at the end of the β-turn in the LexA cleavage loop, we hypothesized that a mutation to proline stabilizes the β-turn and could thereby promote the active conformation of the protein.[54,55] To test this hypothesis, we introduced cysteine mutations at positions A89 and I94, two residues that are within disulfide bonding distance in the active conformation (Figure S2 of the Supporting Information). We then confirmed by mass spectrometry that the variant formed an intramolecular disulfide bond across the β-turn (Figure S8 of the Supporting Information). While the individual point mutants have rates of cleavage slower than (A89C) or comparable to (I94C) that of the wild type, the A89C/I94C double mutant is enhanced, in line with the A92P cleavage rate (Figure 5). While the

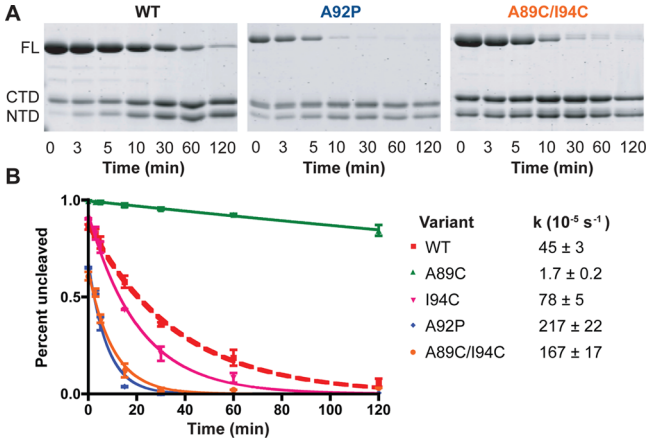

Figure 5. Stabilizing the β-turn around the $LexA_{Pa}$ scissile bond enhances autoproteolysis. (A) Time-dependent cleavage profiles of $LexA_{Pa}$ wild type (WT), A92P, and A89C/I94C. Proteins were incubated at pH 10.6, quenched at the given time points, and visualized using SDS–PAGE. (B) Cleavage kinetics of hyperactive variants and controls with individual mutants to cysteine. In triplicate, the fraction of uncleaved protein was determined using densitometry and fit as a function of time according to first-order decay kinetics.

mechanism cannot be definitively assessed, the A92P and A89C/I94C LexA variants point to the importance of secondary structure formation in the cleavage region, with potential implications for inhibitor design.

DISCUSSION

The emergence of drug resistance in bacterial pathogens is one of the most pressing issues in infectious diseases today, particularly given the limited pipeline of new antimicrobials to combat this threat.[56,57] Given the need for a better mechanistic understanding of bacterial adaptation and novel approaches to combating drug resistance, the idea of targeting the pathways that allow bacterial pathogens to adapt and evolve resistance to

dx.doi.org/10.1021/bi500026e | Biochemistry 2014, 53, 3158–3168

antibiotics has been proposed.[26,30] In support of this approach, stimulating genetic and synthetic biologic studies have suggested that targeting LexA autoproteolysis can prevent activation of the SOS pathway and thereby hypersensitize bacteria to traditional antibiotics, slow acquired drug resistance, and offer insights into the mechanisms driving bacterial evolution. To inform our understanding of LexA, we performed exhaustive mutagenesis studies on >140 variants of LexA that help to delineate the key determinants of proteolysis. These studies have led us to conclude that the LexA repressor-protease possesses a unique substrate preference, with both side-chain and conformational requirements that govern autoproteolysis. Dissecting each of these stringent, intermediate, and tolerant determinants for self-cleavage offers insights into LexA's mechanism (Figure 6) and can fuel future efforts to probe the SOS pathway.

Stringent Determinants: Positions P3, P1, and P1′. We have identified three positions in the LexA cleavage region that are restrictive to extensive mutation. Interestingly, although exhaustive mutagenesis was not performed, point mutations at these positions were also identified to be important for the self-cleavage of the related λ CI repressor, and the positions are well conserved in LexA isoforms across species (Figure 1C).[21] For $LexA_{Pa}$, positions P3 and P1 favor the wild-type residues and show tolerance toward β-branched or small amino acids, respectively. For both positions, analysis of the crystal structure shows extensive van der Waals contacts between the side chains and hydrophobic pockets in the LexA active site (Figure 6B). Because increasing or decreasing the size of the amino acid at these positions reduces cleavage efficiency (Table 1), we conclude that positions P3 and P1 determine specificity through active site contacts.

Position P1′ is the most restrictive position, tolerating only the wild-type glycine and a serine mutation. Position P1′ is located at the end of the β-hairpin turn and undergoes a dramatic bond rotation during the transition between active and inactive conformations.[12] Only glycine can readily adopt and interconvert between these unusual Ramachandran angles, thus explaining the strong preference for the wild-type residue at that position. Larger amino acids likely cause steric clash with the surrounding protein or are hindered in making the necessary bond rotations. Interestingly, trace cleavage was also detectable in the G91S mutant (Figure S6F of the Supporting Information). We speculate that mutation to a serine likely allows for the formation of hydrogen bonds between the side-chain hydroxyl group and peptide backbone that can stabilize the turn, compensating for the decreased level of rotational freedom.

Intermediate Determinants: Positions P5 and P2. Unlike the stringent determinants, positions P5 and P2 tolerate a wide range of mutations yet display a preference for a particular subset of amino acids. At position P5, the wild-type residue, glycine, is preferred over a larger amino acid, such as alanine or serine. Similar to position P1′, in the determined structures of LexA, the glycine at position P5 undergoes a significant rotation during the transition from the inactive state to the active state, thus explaining the presence of a flexible residue that can serve as a molecular hinge.[12]

Position P2 displays an intermediate phenotype, as well: although all variants are tolerated, amino acids that exceed the size of serine decrease the rate of self-cleavage. Structurally, the side chain of position P2 forms contacts with the side chain of position P4′ (I94) located on the opposite side of the loop

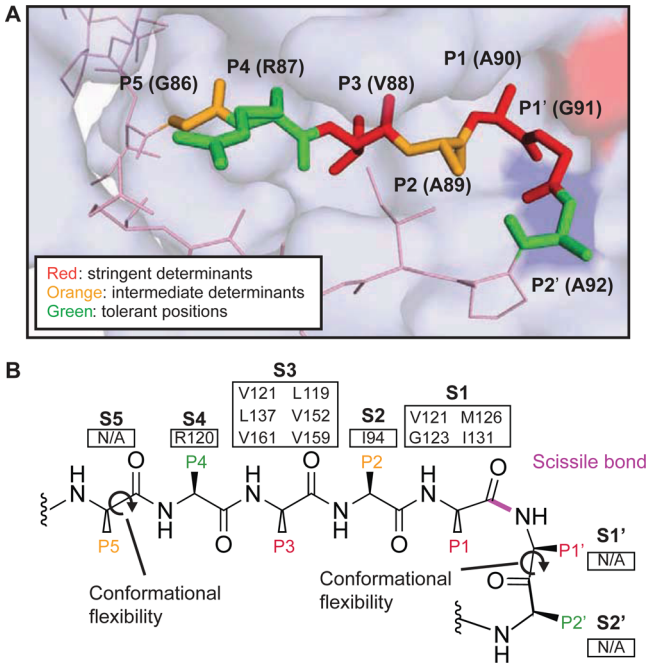

Figure 6. Postulated structure–function relationship of the key residues in the $LexA_{Pa}$ cleavage region. (A) Structural model demonstrating intermediate, stringent, and tolerant positions in the active $LexA_{Pa}$ cleavage region. This active site model is taken from the full homology model of the $LexA_{Pa}$ CTD described in Figure S2 of the Supporting Information. Positions evaluated in this study are shown as sticks and color-coded according to their selectivity (red, stringent; orange, intermediate; green, tolerant). Other residues in the LexA cleavage region are shown as pink lines. The $LexA_{Pa}$ catalytic serine S125 and basic lysine K162 are shaded red and blue, respectively, highlighting the active site. (B) Interactions between the $LexA_{Pa}$ cleavage loop and $LexA_{Pa}$ active site pocket. For each position from position P5 to P2′, the active site residues (S5–S2′) within van der Waals contact range of the side chain are noted in the box. Positions P3 (V88) and P1 (A90) form specific hydrophobic contacts with the surrounding active site, which are conserved in both $LexA_{Pa}$ and $LexA_{Ec}$. Position P2 (A89) interacts with position P4′ (I94) on the opposite side of the loop turn. At each of these positions, the wild-type residues and smaller side chains are more conducive to proteolysis. The two flanking glycines, G86 and G91 (P5 and P1′, respectively), show a preference for the wild-type glycine, which may confer rotational flexibility on the LexA cleavage region, allowing the internal loop to undergo the transition from the inactive form to the active form. Positions P4 (R87) and P2′ (A92), which are notably solvent-exposed, are tolerant to all amino acid substitutions, including several that can enhance cleavage.

(Figure S2 of the Supporting Information). Increasing the size of the amino acid likely reduces the rate of cleavage due to steric clash.

Permissive Positions and Enhanced Autoproteolysis: Positions P4 and P2′. In addition to deciphering specificity determinants, our study has also identified two highly permissive positions that flank the LexA scissile bond. Positions P4 and P2′ can be mutated to the whole amino acid spectrum without abrogating LexA cleavage, although changes in the rate of cleavage are observed. The $LexA_{Pa}$ model structure shows both positions to be relatively solvent-exposed, forming few specific contacts with the surrounding active site. Interestingly, both positions also harbor mutations that enhance the level of self-cleavage compared to that of the wild-type enzyme. At position P4 (R87), mutations removing a basic residue appear

dx.doi.org/10.1021/bi500026e | Biochemistry 2014, 53, 3158–3168

to enhance self-cleavage (Table 1), despite the conservation of the basic residue in LexA across species (Figure 1C). We speculate that these rate-enhancing mutations may result from the removal of a potential repulsive interaction with an adjacent (and well-conserved) positively charged residue (R120) in the active conformation. Position P2′, in contrast to position P4, is highly variable across species (Figure 1C), which correlates well with its tolerance to mutagenesis in our biochemical study. At position P2′, introduction of a proline mutation enhances self-cleavage, likely by stabilizing the β-turn around the scissile bond and thereby promoting the cleavage-competent state of LexA. This model is supported by our analysis of the disulfide cross-linked A89C/I94C mutant, which shows cleavage kinetics similar to those of the A92P mutant (Figure 5B).

Our results expand the list of previously identified mutations that enhance LexA cleavage.[52] In a prior study, mutations located at positions P5′ and P8′ in *E. coli* LexA, distant from the catalytic site, were shown to stabilize the active conformation of the entire LexA cleavage loop.[12,52] Our results for A92P and A89C/I94C mutants suggest that stabilizing the β-turn around the scissile bond with rigid cyclic structures similarly enhances cleavage and could offer novel avenues for inhibitor design.

Conformational Constraints and Side-Chain Recognition in LexA. The nature of our experimental design, which focused on mutations in the cleavage loop and kinetic analysis of autoproteolysis, requires that the enzyme and its substrate change simultaneously. Additionally, given that we evaluated single-point mutants, the impact of combinatorial modifications in the substrate could not be readily assessed from our approach. Despite these limitations, the relative independence of the cleavage loop and the active site residues make it possible to integrate across our biochemical analysis and structural modeling to provide a detailed picture of LexA's specificity. From our analysis, we postulate that the nature of the specificity determinants of LexA can be classified under two broad categories: those permissive for substrate recognition and those permissive for the conformational change in self-cleavage (Figure 6B). Much like conventional proteases, LexA has substrate recognition pockets that determine its selectivity, most evident at positions P3 (V88) and P1 (A90) (Figure 6B). As a key difference from conventional proteases, however, the LexA cleavage region must internally rearrange to adopt a proper cleavage-competent conformation for proteolysis to occur. Positions P5 (G85) and P1′ (G91) are highly dynamic positions, implying that conformational flexibility at either end of the cleavage region appears to be important for autoproteolysis. In support of the importance of dynamic rearrangements in LexA, stabilizing the β-turn across the scissile bond promotes self-cleavage at a level above that of the wild type. We postulate that these requirements for both proper sequence and conformation serve as a mechanism of self-recognition and limit off-target proteolytic activity. Our findings help rationalize the low cleavage activity of the LexA protease *in trans* and offer insights into rational probe design.[18]

Comparison of LexA$_{Pa}$ to Similar Proteases. Our biochemical results are particularly informative when we compare LexA$_{Pa}$ to members of the larger LexA/signal peptidase superfamily, many of which mediate bacterial stress responses (Figure S1B of the Supporting Information). This superfamily includes LexA homologues such as *Bacillus subtilis* DinR and *Vibrio cholerae* SetR, the phage λ CI repressor, and UmuD and MucA, self-cleaving enzymes that function in the SOS-linked translesion DNA synthesis.[11,13,17,18,21,41,58,59] In these enzymes, position P1′ is universally conserved as a glycine (Figure S1 of the Supporting Information), suggesting that the flexibility of position P1′ is likely critical to the mechanism. The stringent residues involved in side-chain contacts are also strongly conserved, with a β-branched residue at position P3 and a small residue at position P1 conserved across comparators (Figure S1B of the Supporting Information). Notably, the position S3 and S1 recognition pockets are entirely conserved between LexA$_{Pa}$ and LexA$_{Ec}$ (Figure S1A of the Supporting Information), suggesting a common mechanism of side-chain recognition in forms of LexA from different species. For the intermediate determinants, the position P5 glycine offers the most revealing comparison to other self-cleaving enzymes. We speculate that this residue is a critical "hinge" for the conformational change that allows self-cleavage within a LexA monomer. Interestingly, position P5 is not conserved in UmuD where cleavage of one monomer can occur in the other monomer's active site.[9] Overall, comparing the superfamily to other common serine proteases, we note that LexA favors small amino acids in the positions flanking the scissile bond, most similar to the elastase family of serine proteases.[23,24] However, the unique self-cleaving mechanism and its conformational requirements are distinguishing features that appear to be well conserved across the LexA/signal peptidase superfamily.

Implications for the Design of Inhibitors and Molecular Probes of LexA. In addition to revealing insights into the mechanism of self-cleavage, several aspects of our substrate specificity studies can potentially help direct future efforts to develop small molecule probes of the SOS pathway. First, while LexA does not have proficient activity with peptides *in trans*, it does have detectable activity. Peptides or peptidomimetics that incorporate preferred features, such as the side chains of positions P3 and P1 or β-turn-stabilizing structures, may be exploited to enhance binding. Even weak binding peptides or peptidomimetics could be converted into more potent probes by the incorporation of mechanism-based covalent inhibitor warheads into such molecules. Second, our discovery of tolerance at positions P4 and P2′ could be exploited in inhibitor discovery. The introduction of fluorescent reporters at these positions could aid in screening for inhibitors of self-cleavage or, given the highly dynamic nature of position P2′, potential allosteric modulators of the conformational change. Finally, our discovery of a range of hypocleavable LexA variants can potentially help further validate LexA's viability as a therapeutic target. Given that LexA inhibitors would be unlikely to fully recapitulate the LexA catalytic mutant, these variants can be used to reveal the amount of inhibition that will be necessary to synergize with current antibiotics or to slow acquired antibiotic resistance.

Implications for Bacterial Mutation and Evolution. We hypothesize that the identification of rate-enhancing mutations by prior genetic studies and our biochemical studies has wider implications for bacterial mutagenesis and evolution.[52,53] The fact that mutations can enhance cleavage suggests the possibility that the rate of LexA autoproteolysis may be finely tuned to be fast enough to facilitate robust SOS responses but slow enough to prevent aberrant SOS pathway activation. This characteristic has been thought to be functionally important in different members of the LexA superfamily. As an example, temperate phage repressors such as the phage λ CI repressor self-cleave more slowly than LexA during SOS-inducing treatments, thereby inducing prophage formation only with

extensive DNA damage.[18] Similarly, mutagenesis proteins, such as UmuD, self-cleave at rates slower than that of LexA, which could promote translesion DNA synthesis later in the SOS response, only after higher-fidelity repair mechanisms have failed.[17] Given that self-cleavage can be either slowed or enhanced by mutations, we hypothesize that the LexA cleavage rate has been selected for to allow for proper activation of the SOS pathway and that LexA may serve as a rheostat for evolution under stress. Our study offers the possibility of modulating the cleavage rates of LexA across a large range to assess the impact on bacterial mutation and survival directly under varying degrees of stress.

■ ASSOCIATED CONTENT

Supporting Information

Alignment of $LexA_{Pa}$ with other superfamily members, structural homology model of $LexA_{Pa}$, functional validation of $LexA_{Pa}$ self-cleavage, overall scheme of the cassette-based mutagenesis, additional screening and kinetic data from all scanning and saturation mutagenesis, and LC−MS/MS data for the $LexA_{Pa}$ A89C/I94C mutant. This material is available free of charge via the Internet at http://pubs.acs.org.

■ AUTHOR INFORMATION

Corresponding Author

*E-mail: rkohli@upenn.edu. Telephone: (215) 573-7523.

Funding

We gratefully acknowledge funding from the National Institutes of Health (NIH Director's New Innovator Award DP2-GM105444 to R.M.K. and Grant K08-AI089242 to R.M.K.). C.Y.M. received support from Cellular and Molecular Biology Training Grant T32 GM7229-36. We also acknowledge funding from the Doris Duke Charitable Foundation, the Edward J. Mallinckrodt, Jr., Foundation, and the Cystic Fibrosis Foundation in support of this research.

Notes

The authors declare no competing financial interest.

■ ACKNOWLEDGMENTS

We thank E. James Petersson and all members of the Kohli laboratory for useful comments. We are grateful to Chao-Xing Yuan of the Penn Proteomics Core for assistance with LC−MS/MS.

■ ABBREVIATIONS

SOS, stress response; $LexA_{Pa}$, *P. aeruginosa* LexA; $LexA_{Ec}$, *E. coli* LexA; NTD, N-terminal DNA binding domain; CTD, C-terminal serine protease domain; RecA*, activated RecA; NEB, New England Biolabs; IDT, Integrated DNA Technologies; LC−MS/MS, liquid chromatography and tandem mass spectrometry; PDB, Protein Data Bank.

■ REFERENCES

(1) Sutton, M. D., Smith, B. T., Godoy, V. G., and Walker, G. C. (2000) The SOS response: Recent insights into umuDC-dependent mutagenesis and DNA damage tolerance. *Annu. Rev. Genet. 34*, 479−497.

(2) Michel, B. (2005) After 30 years of study, the bacterial SOS response still surprises us. *PLoS Biol. 3*, e255.

(3) Schlacher, K., and Goodman, M. F. (2007) Lessons from 50 years of SOS DNA-damage-induced mutagenesis. *Nat. Rev. Mol. Cell Biol. 8*, 587−594.

(4) Courcelle, J., Khodursky, A., Peter, B., Brown, P. O., and Hanawalt, P. C. (2001) Comparative gene expression profiles following UV exposure in wild-type and SOS-deficient *Escherichia coli*. *Genetics 158*, 41−64.

(5) Galhardo, R. S., Do, R., Yamada, M., Friedberg, E. C., Hastings, P. J., Nohmi, T., and Rosenberg, S. M. (2009) DinB upregulation is the sole role of the SOS response in stress-induced mutagenesis in *Escherichia coli*. *Genetics 182*, 55−68.

(6) Boshoff, H. I., Reed, M. B., Barry, C. E., III, and Mizrahi, V. (2003) DnaE2 polymerase contributes to in vivo survival and the emergence of drug resistance in *Mycobacterium tuberculosis*. *Cell 113*, 183−193.

(7) Guerin, E., Cambray, G., Sanchez-Alberola, N., Campoy, S., Erill, I., Da Re, S., Gonzalez-Zorn, B., Barbe, J., Ploy, M. C., and Mazel, D. (2009) The SOS response controls integron recombination. *Science 324*, 1034.

(8) Gotoh, H., Kasaraneni, N., Devineni, N., Dallo, S. F., and Weitao, T. (2010) SOS involvement in stress-inducible biofilm formation. *Biofouling 26*, 603−611.

(9) McDonald, J. P., Peat, T. S., Levine, A. S., and Woodgate, R. (1999) Intermolecular cleavage by UmuD-like enzymes: Identification of residues required for cleavage and substrate specificity. *J. Mol. Biol. 285*, 2199−2209.

(10) Slilaty, S. N., Rupley, J. A., and Little, J. W. (1986) Intramolecular cleavage of LexA and phage lambda repressors: Dependence of kinetics on repressor concentration, pH, temperature, and solvent. *Biochemistry 25*, 6866−6875.

(11) Burckhardt, S. E., Woodgate, R., Scheuermann, R. H., and Echols, H. (1988) UmuD mutagenesis protein of *Escherichia coli*: Overproduction, purification, and cleavage by RecA. *Proc. Natl. Acad. Sci. U.S.A. 85*, 1811−1815.

(12) Luo, Y., Pfuetzner, R. A., Mosimann, S., Paetzel, M., Frey, E. A., Cherney, M., Kim, B., Little, J. W., and Strynadka, N. C. (2001) Crystal structure of LexA: A conformational switch for regulation of self-cleavage. *Cell 106*, 585−594.

(13) Cezairliyan, B. O., and Sauer, R. T. (2009) Control of *Pseudomonas aeruginosa* AlgW protease cleavage of MucA by peptide signals and MucB. *Mol. Microbiol. 72*, 368−379.

(14) Little, J. W. (1984) Autodigestion of lexA and phage lambda repressors. *Proc. Natl. Acad. Sci. U.S.A. 81*, 1375−1379.

(15) Slilaty, S. N., and Little, J. W. (1987) Lysine-156 and serine-119 are required for LexA repressor cleavage: A possible mechanism. *Proc. Natl. Acad. Sci. U.S.A. 84*, 3987−3991.

(16) Zhang, A. P., Pigli, Y. Z., and Rice, P. A. (2010) Structure of the LexA-DNA complex and implications for SOS box measurement. *Nature 466*, 883−886.

(17) Nohmi, T., Battista, J. R., Dodson, L. A., and Walker, G. C. (1988) RecA-mediated cleavage activates UmuD for mutagenesis: Mechanistic relationship between transcriptional derepression and posttranslational activation. *Proc. Natl. Acad. Sci. U.S.A. 85*, 1816−1820.

(18) Kim, B., and Little, J. W. (1993) LexA and lambda cI repressors as enzymes: Specific cleavage in an intermolecular reaction. *Cell 73*, 1165−1173.

(19) Shepley, D. P., and Little, J. W. (1996) Mutant LexA proteins with specific defects in autodigestion. *Proc. Natl. Acad. Sci. U.S.A. 93*, 11528−11533.

(20) Lin, L. L., and Little, J. W. (1988) Isolation and characterization of noncleavable (ind-) mutants of the LexA repressor of *Escherichia coli* K-12. *J. Bacteriol. 170*, 2163−2173.

(21) Gimble, F. S., and Sauer, R. T. (1985) Mutations in bacteriophage lambda repressor that prevent RecA-mediated cleavage. *J. Bacteriol. 162*, 147−154.

(22) Tyndall, J. D., Nall, T., and Fairlie, D. P. (2005) Proteases universally recognize β strands in their active sites. *Chem. Rev. 105*, 973−999.

(23) Perona, J. J., and Craik, C. S. (1995) Structural basis of substrate specificity in the serine proteases. *Protein Sci. 4*, 337−360.

(24) Hedstrom, L. (2002) Serine protease mechanism and specificity. *Chem. Rev. 102*, 4501−4524.
(25) Roland, K. L., and Little, J. W. (1990) Reaction of LexA repressor with diisopropyl fluorophosphate. A test of the serine protease model. *J. Biol. Chem. 265*, 12828−12835.
(26) Cirz, R. T., Chin, J. K., Andes, D. R., de Crecy-Lagard, V., Craig, W. A., and Romesberg, F. E. (2005) Inhibition of mutation and combating the evolution of antibiotic resistance. *PLoS Biol. 3*, e176.
(27) Lu, T. K., and Collins, J. J. (2009) Engineered bacteriophage targeting gene networks as adjuvants for antibiotic therapy. *Proc. Natl. Acad. Sci. U.S.A. 106*, 4629−4634.
(28) Dorr, T., Lewis, K., and Vulic, M. (2009) SOS response induces persistence to fluoroquinolones in *Escherichia coli*. *PLoS Genet. 5*, e1000760.
(29) Al Mamun, A. A., Lombardo, M. J., Shee, C., Lisewski, A. M., Gonzalez, C., Lin, D., Nehring, R. B., Saint-Ruf, C., Gibson, J. L., Frisch, R. L., Lichtarge, O., Hastings, P. J., and Rosenberg, S. M. (2012) Identity and function of a large gene network underlying mutagenic repair of DNA breaks. *Science 338*, 1344−1348.
(30) Smith, P. A., and Romesberg, F. E. (2007) Combating bacteria and drug resistance by inhibiting mechanisms of persistence and adaptation. *Nat. Chem. Biol. 3*, 549−556.
(31) Cirz, R. T., and Romesberg, F. E. (2007) Controlling mutation: Intervening in evolution as a therapeutic strategy. *Crit. Rev. Biochem. Mol. Biol. 42*, 341−354.
(32) Lyczak, J. B., Cannon, C. L., and Pier, G. B. (2002) Lung infections associated with cystic fibrosis. *Clin. Microbiol. Rev. 15*, 194−222.
(33) Folkesson, A., Jelsbak, L., Yang, L., Johansen, H. K., Ciofu, O., Hoiby, N., and Molin, S. (2012) Adaptation of *Pseudomonas aeruginosa* to the cystic fibrosis airway: An evolutionary perspective. *Nat. Rev. Microbiol. 10*, 841−851.
(34) Jacobs, M. A., Alwood, A., Thaipisuttikul, I., Spencer, D., Haugen, E., Ernst, S., Will, O., Kaul, R., Raymond, C., Levy, R., Chun-Rong, L., Guenthner, D., Bovee, D., Olson, M. V., and Manoil, C. (2003) Comprehensive transposon mutant library of *Pseudomonas aeruginosa*. *Proc. Natl. Acad. Sci. U.S.A. 100*, 14339−14344.
(35) Tracy, R. B., and Kowalczykowski, S. C. (1996) In vitro selection of preferred DNA pairing sequences by the *Escherichia coli* RecA protein. *Genes Dev. 10*, 1890−1903.
(36) Workman, C. T., Yin, Y., Corcoran, D. L., Ideker, T., Stormo, G. D., and Benos, P. V. (2005) enoLOGOS: A versatile web tool for energy normalized sequence logos. *Nucleic Acids Res. 33*, W389−W392.
(37) Sali, A., and Blundell, T. L. (1993) Comparative protein modelling by satisfaction of spatial restraints. *J. Mol. Biol. 234*, 779−815.
(38) Ma, B., Zhang, K., Hendrie, C., Liang, C., Li, M., Doherty-Kirby, A., and Lajoie, G. (2003) PEAKS: Powerful software for peptide de novo sequencing by tandem mass spectrometry. *Rapid Commun. Mass Spectrom. 17*, 2337−2342.
(39) Movahedzadeh, F., Colston, M. J., and Davis, E. O. (1997) Characterization of *Mycobacterium tuberculosis* LexA: Recognition of a cheo (*Bacillus*-type SOS) box. *Microbiology 143* (Part 3), 929−936.
(40) Cohn, M. T., Kjelgaard, P., Frees, D., Penades, J. R., and Ingmer, H. (2011) Clp-dependent proteolysis of the LexA N-terminal domain in *Staphylococcus aureus*. *Microbiology 157*, 677−684.
(41) Miller, M. C., Resnick, J. B., Smith, B. T., and Lovett, C. M., Jr. (1996) The *Bacillus subtilis* dinR gene codes for the analogue of *Escherichia coli* LexA. Purification and characterization of the DinR protein. *J. Biol. Chem. 271*, 33502−33508.
(42) Giese, K. C., Michalowski, C. B., and Little, J. W. (2008) RecA-dependent cleavage of LexA dimers. *J. Mol. Biol. 377*, 148−161.
(43) Salisbury, C. M., Maly, D. J., and Ellman, J. A. (2002) Peptide microarrays for the determination of protease substrate specificity. *J. Am. Chem. Soc. 124*, 14868−14870.
(44) Van Damme, P., Vandekerckhove, J., and Gevaert, K. (2008) Disentanglement of protease substrate repertoires. *Biol. Chem. 389*, 371−381.
(45) O'Donoghue, A. J., Eroy-Reveles, A. A., Knudsen, G. M., Ingram, J., Zhou, M., Statnekov, J. B., Greninger, A. L., Hostetter, D. R., Qu, G., Maltby, D. A., Anderson, M. O., Derisi, J. L., McKerrow, J. H., Burlingame, A. L., and Craik, C. S. (2012) Global identification of peptidase specificity by multiplex substrate profiling. *Nat. Methods 9*, 1095−1100.
(46) Harris, J. L., Backes, B. J., Leonetti, F., Mahrus, S., Ellman, J. A., and Craik, C. S. (2000) Rapid and general profiling of protease specificity by using combinatorial fluorogenic substrate libraries. *Proc. Natl. Acad. Sci. U.S.A. 97*, 7754−7759.
(47) Schilling, O., and Overall, C. M. (2008) Proteome-derived, database-searchable peptide libraries for identifying protease cleavage sites. *Nat. Biotechnol. 26*, 685−694.
(48) Reidhaar-Olson, J. F., and Sauer, R. T. (1988) Combinatorial cassette mutagenesis as a probe of the informational content of protein sequences. *Science 241*, 53−57.
(49) Davidson, A. R., Lumb, K. J., and Sauer, R. T. (1995) Cooperatively folded proteins in random sequence libraries. *Nat. Struct. Biol. 2*, 856−864.
(50) Bowie, J. U., Reidhaar-Olson, J. F., Lim, W. A., and Sauer, R. T. (1990) Deciphering the message in protein sequences: Tolerance to amino acid substitutions. *Science 247*, 1306−1310.
(51) Lin, L. L., and Little, J. W. (1989) Autodigestion and RecA-dependent cleavage of ind- mutant LexA proteins. *J. Mol. Biol. 210*, 439−452.
(52) Smith, M. H., Cavenagh, M. M., and Little, J. W. (1991) Mutant LexA proteins with an increased rate of in vivo cleavage. *Proc. Natl. Acad. Sci. U.S.A. 88*, 7356−7360.
(53) Roland, K. L., Smith, M. H., Rupley, J. A., and Little, J. W. (1992) In vitro analysis of mutant LexA proteins with an increased rate of specific cleavage. *J. Mol. Biol. 228*, 395−408.
(54) Trevino, S. R., Schaefer, S., Scholtz, J. M., and Pace, C. N. (2007) Increasing protein conformational stability by optimizing β-turn sequence. *J. Mol. Biol. 373*, 211−218.
(55) Fu, H., Grimsley, G. R., Razvi, A., Scholtz, J. M., and Pace, C. N. (2009) Increasing protein stability by improving β-turns. *Proteins 77*, 491−498.
(56) Fischbach, M. A., and Walsh, C. T. (2009) Antibiotics for emerging pathogens. *Science 325*, 1089−1093.
(57) Clatworthy, A. E., Pierson, E., and Hung, D. T. (2007) Targeting virulence: A new paradigm for antimicrobial therapy. *Nat. Chem. Biol. 3*, 541−548.
(58) Shiba, T., Iwasaki, H., Nakata, A., and Shinagawa, H. (1990) Proteolytic processing of MucA protein in SOS mutagenesis: Both processed and unprocessed MucA may be active in the mutagenesis. *Mol. Gen. Genet. 224*, 169−176.
(59) Beaber, J. W., Hochhut, B., and Waldor, M. K. (2004) SOS response promotes horizontal dissemination of antibiotic resistance genes. *Nature 427*, 72−74.